Coupled cluster evaluation of the second and third harmonic scattering responses of small molecules

Beaujean, Pierre; Champagne, Benoît

Published in:
Theoretical Chemistry Accounts

DOI:
10.1007/s00214-018-2219-y

Publication date:
2018

Document Version
Publisher's PDF, also known as Version of record

Theoretical Chemistry Accounts (2018) 137:50
https://doi.org/10.1007/s00214-018-2219-y

REGULAR ARTICLE

Coupled cluster evaluation of the second and third harmonic scattering responses of small molecules

Pierre Beaujean[1] · **Benoît Champagne**[1]

Received: 10 October 2017 / Accepted: 28 December 2017

Abstract
The static and dynamic second harmonic (β_{SHS}) and third harmonic (γ_{THS}) scattering hyperpolarizabilities and depolarization ratios of water, carbon tetrachloride, chloroform, dichloromethane, chloromethane, and acetonitrile have been evaluated at the coupled cluster response theory level of approximation. Following two recent publications on their measurements, this is the first quantum chemical investigation on γ_{THS} and on its decomposition into its spherical tensor components. Substantial electron correlation and basis set effects are evidenced for β_{SHS} and γ_{THS} and for their depolarization ratios, and they depend on the nature of the molecule. Then, using the selected CCSD/d-aug-cc-pVDZ level, the chlorinated methane derivatives have been studied, showing that (i) the γ_{THS} response is dominated by its isotropic contribution, whereas (ii) for β_{SHS} the dipolar contribution increases from carbon tetrachloride to dichloromethane, chloroform, chloromethane, and acetonitrile. Comparisons with the experimental data obtained from measurements in liquid phase (i) show that the increase of γ_{THS} with the number for chlorine atoms is well reproduced by the calculations and (ii) suggest that the solvation effects are smaller for γ_{THS} than for β_{SHS}.

Keywords First and second hyperpolarizabilities · Coupled cluster response functions · Second and third harmonic scattering

1 Introduction

Since the first observation of the second harmonic generation (SHG) phenomenon by Franken et al. [1] in 1961 and of the third harmonic generation (THG) phenomenon, one year later by Terhune et al. [2], these phenomena have been exploited to understand the properties of molecules and their interactions with electro-magnetic fields [3]. In parallel, the development of accurate theoretical methods has provided complementary tools for the evaluation of the corresponding molecular properties, the first (β) and the second (γ) hyperpolarizabilities [4–10]. This has led to the deduction of the necessary structure-NLO (nonlinear optical) property relationships to design molecules with large β and γ responses as well as interpretation tools when these properties are used to probe the structures, properties, and dynamics of molecules and matter.

Recently, Van Steerteghem et al. [11] and Rodriguez [12] have shown that γ can also be determined from Third Harmonic Scattering (THS) measurements, opening a new direction for investigating structure-γ relationships as well as to assess the potential of THS γ as a probe of molecular structures and properties. THS technique is the next-order analog of second harmonic scattering (SHS), usually called hyper-Rayleigh scattering (HRS), which has already permitted β measurements for a broad range of molecules and ions [13–16, 45], including organic and organometallic compounds as well as, more recently, molecular switches [3, 17–24].

Published as part of the special collection of articles "Festschrift in honour of A. Rizzo".

Electronic supplementary material The online version of this article (https://doi.org/10.1007/s00214-018-2219-y) contains supplementary material, which is available to authorized users.

✉ Benoît Champagne
benoit.champagne@unamur.be

Pierre Beaujean
pierre.beaujean@unamur.be

[1] Laboratory of Theoretical Chemistry, Unit of Theoretical and Structural Physical Chemistry, Namur Institute of Structured Matter, University of Namur, rue de Bruxelles 61, B-5000 Namur, Belgium

Published online: 07 March 2018

In most cases, both SHS and THS experimental determinations of β and γ rely on relative rather than on absolute measurements, which requires a precise knowledge of the responses of these reference compounds, typically small molecules [3, 6, 25]. As shown over the last decades, the definition of reference values results often from joint experimental and theoretical/quantum chemical investigations. On the one hand, the small size of these reference compounds allows using high-level methods (extended basis sets, high-order electron correlation treatment, vibrational contributions, effects of the surrounding) [26–36]. On the other hand, they allow assessing the reliability of more approximate methods. For instance, Castet et al. [37, 38] have reported experimental SHS results (on β and its depolarization ratio) of five small molecules in solution and have discussed the performance of various *ab initio* methods to reproduce qualitatively and quantitatively the experimental data.

In this paper, a hierarchy of coupled cluster (CC) methods is employed to perform the first quantum chemistry investigation of the THS responses of reference molecules. The present study follows two recent contributions of our group [39, 40] on other NLO responses. Six molecules have been selected: water (H_2O), chloromethane (CH_3Cl), dichloromethane (CH_2Cl_2), chloroform ($CHCl_3$), carbon tetrachloride (CCl_4), and acetonitrile (CH_3CN). H_2O has been chosen because its small size enables a detailed investigation of basis set and electron correlation effects, as we demonstrated in a recent paper [40]. The other molecules enable to unravel the effect of molecular symmetry on the THS response: CCl_4 belongs to the $\mathbf{T}_d$ point group, CH_3Cl, $CHCl_3$, and CH_3CN belong to C_{3v}, while CH_2Cl_2 (and H_2O) to C_{2v}. Note also that the later four compounds have already been studied experimentally by THS in Refs. [11, 12] and by SHS in Ref. [37]. Besides γ_{THS}, for the sake of completeness, the present study also reports the β_{SHS} results. Then, only the electronic contribution to the first and second hyperpolarizabilities is computed. In the case of second harmonic generation β and third harmonic generation γ, the pure vibrational contributions are indeed expected to be small at optical frequencies [41, 42] whereas considering the zero-point vibrational average is beyond the scope of this investigation.

This paper is divided in four sections: (1) Sect. 2 gives a short description of SHS and THS methods and their target quantities; (2) the computational details are presented in Sect. 3; (3) the main results are presented and analyzed in Sect. 4: first, the electron correlation and basis set effects are investigated on the static first and second hyperpolarizabilities of the water molecule and then on the frequency dispersion of the second- and third-order scattering responses of acetonitrile. Then, a selected method is employed to study the static and dynamic SHS and THS hyperpolarizabilities of the four other molecules; (4) the conclusions are drawn in Sect. 5.

2 The SHS and THS spectroscopies

At the molecular scale, the frequency-dependent first and second hyperpolarizabilities are the expansion coefficients of the molecular induced dipole moment as a function of external electric fields, $\mathbf{F}$, applied along the i, j, ...directions (note that lower-case letters stand for coordinates in the molecular frame) and oscillating at frequencies ω_1, ω_2, ...:

$$\begin{aligned}\Delta\mu_i(\mathbf{F}) = &\sum_{j}^{x,y,z} \alpha_{ij}(-\omega_\sigma;\omega_1)\, F_j(\omega_1) \\ &+ \frac{1}{2!}\sum_{jk}^{x,y,z} \beta_{ijk}(-\omega_\sigma;\omega_1,\omega_2)\, F_j(\omega_1)\, F_k(\omega_2) \\ &+ \frac{1}{3!}\sum_{jkl}^{x,y,z} \gamma_{ijkl}(-\omega_\sigma;\omega_1,\omega_2,\omega_3)\, F_j(\omega_1)\; F_k(\omega_2)\, F_l(\omega_3) \\ &+ \ldots\end{aligned} \tag{1}$$

where $\omega_\sigma = \sum_i \omega_i$, α_{ij} is an element of the polarizability tensor, while β_{ijk} and γ_{ijkl} are elements of the first and second hyperpolarizability tensors, respectively. Depending on the combination of static and dynamic electric fields, different NLO processes arise. The second and third harmonic generation responses are noted $\beta(-2\omega;\omega,\omega)$ and $\gamma(-3\omega;\omega,\omega,\omega)$, respectively.

For an isotropic medium composed of identical molecules or scatterers, the intensity of incoherent contribution to the harmonic scattered light $I^{m\omega}$ reads :

$$I^{m\omega} = G f_L^2\, C\langle\chi^2\rangle\, (I^{\omega})^m, \tag{2}$$

where $I^{m\omega}$ is the light intensity at the second ($m = 2$) or third ($m = 3$) harmonic, I^{ω} is the incident intensity, G is a constant containing geometrical, optical, and electrical factors of the experimental setup, C is the scatterers concentration, χ is either β or γ, and f_L is a local field correction depending on the refractive indices of the medium at frequencies ω and $m\omega$. The brackets refer to an isotropic (or rotational) averaging of the tensor over all possible molecular orientations [3, 12, 37, 43].

In the conventional experimental setup (Fig. 1), the scattered light is analyzed at a 90° angle with respect to the direction of propagation. So, the fundamental light beam (of frequency ω), which is elliptically polarized (Ψ and δ describe the state of polarization, and in this case $\delta = \frac{\pi}{2}$), propagates in the Y direction, while the Z-linearly polarized component of the scattered beam (of frequency $m\omega$) is recorded in the X direction. One generally distinguishes between two polarization combinations: the VV geometry (vertical–vertical, both incident and scattered lights are vertically polarized, with $\Psi = \frac{\pi}{2}$) and HV [horizontal–vertical, the incident (scattered) light is horizontally(vertically)-polarized, with $\Psi = 0$]. For SHS and

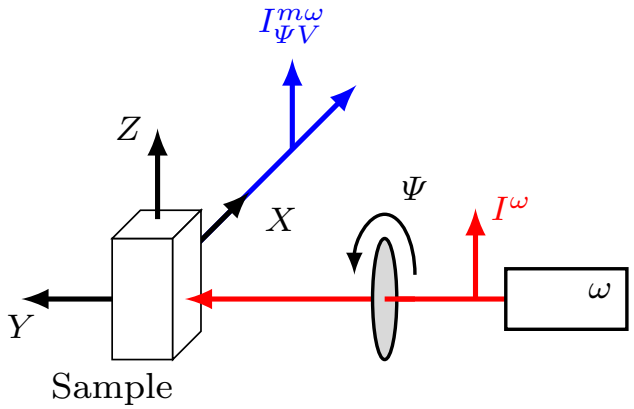

Fig. 1 Sketch of the experimental SHS ($m\omega = 2\omega$) and THS ($m\omega = 3\omega$) setup [3, 12, 14, 43]. *X*, *Y* and *Z* stand for the coordinates axes in the laboratory frame

THS, the I_{VV} intensity is proportional to $\langle\beta^2_{ZZZ}\rangle$ and $\langle\gamma^2_{ZZZZ}\rangle$, while I_{HV} is proportional to $\langle\beta^2_{ZXX}\rangle$ and $\langle\gamma^2_{ZXXX}\rangle$, respectively. The expressions for those averages can be derived following the technique described by Andrew and Thirunamachandran [44]. For SHS [45–47], the resulting expressions are:

$$\langle\beta^2_{ZZZ}\rangle = \frac{1}{105}\sum_{ijk}^{x,y,z}\left\{\begin{array}{l} 2\,\beta^2_{ijk} + \beta_{ijj}\beta_{ikk} \\ +4\,\beta_{iij}\beta_{jkk} + 4\,\beta_{iij}\beta_{kkj} \\ +4\,\beta_{ijk}\beta_{jik} \end{array}\right\}, \tag{3}$$

$$\langle\beta^2_{ZXX}\rangle = \frac{1}{105}\sum_{ijk}^{x,y,z}\left\{\begin{array}{l} 6\,\beta^2_{ijk} + 3\,\beta_{ijj}\beta_{ikk} \\ -2\,\beta_{iij}\beta_{jkk} - 2\,\beta_{iij}\beta_{kkj} \\ -2\,\beta_{ijk}\beta_{jik} \end{array}\right\}, \tag{4}$$

while for THS they read:

$$\langle\gamma^2_{ZZZZ}\rangle = \frac{1}{315}\sum_{ijkl}^{x,y,z}\left\{\begin{array}{l} 2\,\gamma^2_{ijkl} + 12\,\gamma_{iijk}\gamma_{jllk} \\ +6\,\gamma_{iijk}\gamma_{ljlk} + 6\,\gamma_{ijkl}\gamma_{jikl} \\ +3\,\gamma_{iijk}\gamma_{ikll} + 3\,\gamma_{iijj}\gamma_{kllk} \\ +3\,\gamma_{iijk}\gamma_{kill} \end{array}\right\}, \tag{5}$$

$$\langle\gamma^2_{ZXXX}\rangle = \frac{1}{630}\sum_{ijkl}^{x,y,z}\left\{\begin{array}{l} 16\,\gamma^2_{ijkl} + 24\,\gamma_{iijk}\gamma_{ikll} \\ -12\,\gamma_{iijk}\gamma_{jllk} - 6\,\gamma_{iijk}\gamma_{ljlk} \\ -6\,\gamma_{ijkl}\gamma_{jikl} - 3\,\gamma_{iijj}\gamma_{kllk} \\ -3\,\gamma_{iijk}\gamma_{kill} \end{array}\right\}. \tag{6}$$

Note that these expressions undergo simplifications if Kleinman's conditions (full permutation of the tensors components) are assumed (see below). For a non-polarized incident signal, both polarizations have equal probability and the intensity becomes proportional to the sum of the HV and VV observables. This allows defining β_{SHS} and γ_{THS}:

$$\beta_{SHS} = \sqrt{\langle\beta^2_{ZZZ}\rangle + \langle\beta^2_{ZXX}\rangle}, \tag{7}$$

$$\gamma_{THS} = \sqrt{\langle\gamma^2_{ZZZZ}\rangle + \langle\gamma^2_{ZXXX}\rangle}, \tag{8}$$

and their associated depolarization ratios (DR):

$$DR = \frac{I_{VV}}{I_{HV}} \Rightarrow DR_{SHS} = \frac{\langle\beta^2_{ZZZ}\rangle}{\langle\beta^2_{ZXX}\rangle}, \tag{9}$$

$$\Rightarrow DR_{THS} = \frac{\langle\gamma^2_{ZZZZ}\rangle}{\langle\gamma^2_{ZXXX}\rangle}. \tag{10}$$

To further analyze the β and γ tensors, they are decomposed into their irreducible spherical components [48]. These analyses have been pioneered by Kielich et al. [49, 50] and later on used by Brasselet and Zyss [51] for SHS. When assuming the Kleinman's conditions, β contains a dipolar ($J = 1$) and an octupolar ($J = 3$) component [51], expressed as:

$$|\beta_{J=1}|^2 = \frac{3}{5}\sum_{ijk}^{x,y,z}\beta_{ijj}\beta_{ikk}, \tag{11}$$

$$|\beta_{J=3}|^2 = \sum_{ijk}^{x,y,z}\beta^2_{ijk} - \frac{3}{5}\beta_{ijj}\beta_{ikk}. \tag{12}$$

Consequently, in the static limit, the averaged β quantities (Eqs. 3 and 4 can be rewritten under the following form:

$$\langle\beta^2_{ZZZ}\rangle = \frac{9}{45}\,|\beta_{J=1}|^2 + \frac{6}{105}\,|\beta_{J=3}|^2, \tag{13}$$

$$\langle\beta^2_{ZXX}\rangle = \frac{1}{45}\,|\beta_{J=1}|^2 + \frac{4}{105}\,|\beta_{J=3}|^2. \tag{14}$$

A β-nonlinear anisotropy parameter, $\rho_{3/1} = \frac{|\beta_{J=3}|}{|\beta_{J=1}|}$, can also be defined to highlight whether the first hyperpolarizability is dominated by dipolar or octupolar contributions. The depolarization ratio is then rewritten as a function of $\rho_{3/1}$:

$$DR_{SHS} = \frac{18\,\rho^2_{3/1} + 63}{12\,\rho^2_{3/1} + 7}, \tag{15}$$

so that, if the NLOphore is purely dipolar ($\rho_{3/1} \to 0$), the depolarization ratio is equal to 9, while it amounts to $\frac{3}{2}$ if it is purely octupolar ($\rho_{3/1} \to \infty$).

On the other hand, the static γ tensor is composed of an isotropic ($J = 0$), a quadrupolar ($J = 2$), and a hexadecapolar ($J = 4$) spherical tensor component [50], with:

$$|\gamma_{J=0}|^2 = \frac{1}{5} \sum_{ijkl}^{x,y,z} \gamma_{iijj}\gamma_{kkll}, \tag{16}$$

$$|\gamma_{J=2}|^2 = \frac{1}{7} \sum_{ijkl}^{x,y,z} 6\,\gamma_{iijk}\gamma_{jkll} - 2\,\gamma_{iijj}\gamma_{kkll}, \tag{17}$$

$$|\gamma_{J=4}|^2 = \frac{1}{35} \sum_{ijkl}^{x,y,z} 35\gamma_{ijkl}^2 - 30\,\gamma_{iijk}\gamma_{jkll} + 3\,\gamma_{iijj}\gamma_{kkll}. \tag{18}$$

This allows rewriting the expressions for the average γ quantities (Eqs. 5, 6) [50]:

$$\langle\gamma_{ZZZZ}^2\rangle = \frac{1}{5}|\gamma_{J=0}|^2 + \frac{4}{35}|\gamma_{J=2}|^2 + \frac{8}{315}|\gamma_{J=4}|^2, \tag{19}$$

$$\langle\gamma_{ZXXX}^2\rangle = \frac{3}{140}|\gamma_{J=2}|^2 + \frac{1}{63}|\gamma_{J=4}|^2, \tag{20}$$

showing there is no isotropic contribution to $\langle\gamma_{ZXXX}^2\rangle$. The γ-nonlinear anisotropy parameters, $\rho_{0/2} = \frac{|\gamma_{J=0}|}{|\gamma_{J=2}|}$ and $\rho_{4/2} = \frac{|\gamma_{J=4}|}{|\gamma_{J=2}|}$, compare the relative contributions of the different components of the second hyperpolarizability tensor with each other. Note that these definitions differ from those of Rodriguez [12] (which, using the same notations, would be written $\rho_{2/0}$ and $\rho_{4/0}$). Our choice was motivated by the fact that the isotropic contribution is generally larger than the two other ones, resulting in nonlinear anisotropy parameters $\ll 1$ (*vide infra*). In this new framework, the THS depolarization ratio (Eq. 10) is rewritten as:

$$\mathrm{DR}_{\mathrm{THS}} = \frac{32\,\rho_{4/2}^2 + 252\,\rho_{0/2}^2 + 144}{20\,\rho_{4/2}^2 + 27}. \tag{21}$$

The evolution of $\mathrm{DR}_{\mathrm{THS}}$ as a function of $\rho_{4/2}$ for different values of $\rho_{0/2}$ is plotted in Fig. 2. When $\rho_{4/2} \to \infty$, $\mathrm{DR}_{\mathrm{THS}}$ converges to the hexadecapolar limit, $\frac{8}{5}$. However, when $\rho_{4/2} \to 0$ (left part of Fig. 2), the limit value depends on $\rho_{0/2}$, since

$$\mathrm{DR'}_{\mathrm{THS}} = \lim_{\rho_{4/2}\to 0} \mathrm{DR}_{\mathrm{THS}} = \frac{28}{3}\rho_{0/2}^2 + \frac{16}{3}, \tag{22}$$

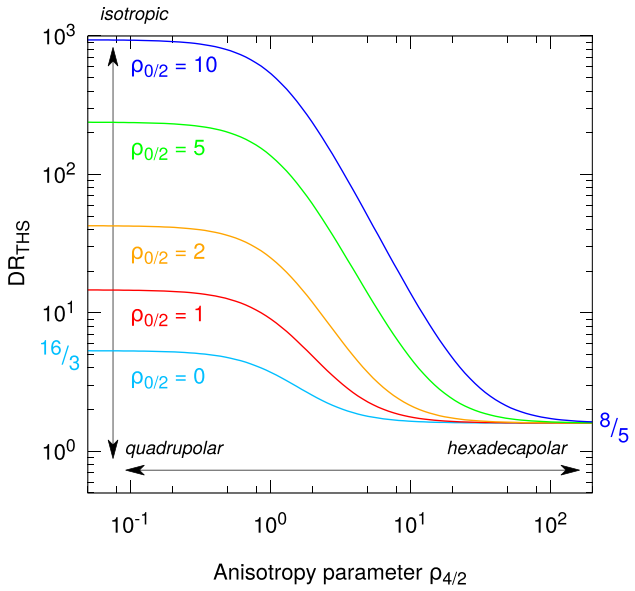

Fig. 2 Evolution of the THS depolarization ratio as a function of $\rho_{4/2}$ for different values of $\rho_{0/2}$. A logarithmic scale is used. When $\rho_{4/2}$ increases, the curves tend to the hexadecapolar limit (8/5), while the quadrupolar limit (16/3) is visible at the beginning of the curve for $\rho_{0/2} = 0$ (see text for more details)

so that the depolarization ratio tends to the "pure" quadrupolar limit of $\frac{16}{3}$ when $\rho_{0/2} \to 0$, and to ∞ when $\rho_{0/2} \to \infty$, *i.e.,* in the isotropic limit.

3 Computational methodology

For the water molecule, the geometry from Ref. [40] was used to facilitate the comparison with previous results on electric field-induced second harmonic generation (EFISHG) quantities. The geometry of the five other molecules was optimized at the MP2/cc-pVTZ level of approximation. Static first and second hyperpolarizabilities were computed with the Dalton 2016 program [52] with a hierarchy of coupled clusters (CC) methods in combination with the quadratic/cubic response function approaches [53–56]. Unrelaxed orbitals were assumed. The employed CC hierarchy, given in increasing order of electron correlation content, is HF, CCS, CC2, and CCSD [53–56]. Following the results of a previous investigation on related properties showing that CCSD and CC3 results are very close [40], no attempt was made to go beyond CCSD. The correlation consistent polarized valence basis sets of Dunning [57], singly or doubly augmented with diffuse functions, (d-)aug-cc-pVXZ, were employed, in a consistent way with respect to previous investigations on small reference molecules for nonlinear optics [37, 39, 40]. Both static and dynamic quantities were calculated. Wavelengths of 1500, 1300 (typical for γ_{THS}), and

1064 nm (typical for β_{SHS}) were selected to analyze the frequency dispersion of β and γ using the following frequency dispersion factor:

$$D\left(\omega_L^2\right) = \frac{\chi(\omega_\sigma;\omega_1,\ldots)}{\chi(0)} - 1, \qquad \text{with } \omega_L^2 = \sum_i^{\sigma,1,\ldots} \omega_i^2 \qquad (23)$$

where χ is either β or γ and $\chi(0)$ is the corresponding static value. All reported β and γ values are given in a.u. [1 a.u. of $\beta = 3.6212 \times 10^{-42}$ m^4 V^{-1} $= 3.2064 \times 10^{-53}$ C^3 m^3 J^{-2} $= 8.639 \times 10^{-33}$ esu; 1 a.u. of $\gamma = 7.423 \times 10^{-54}$ m^5 V^{-2} $= 6.2354 \times 10^{-65}$C^4 m^4 J^{-3} $= 5.0367 \times 10^{-40}$ esu] and within the T-convention.

4 Results and discussion

4.1 Basis sets and electron correlation effects

The SHS and THS responses of water and acetonitrile molecules were calculated first in order to investigate the basis sets and electron correlation effects. For water, the results are reported in Table 1 for the static first and second hyperpolarizabilities, and they are summarized in Fig. 3. The convergence with the size of the basis set is fast for β_{SHS}. At the four levels of approximation considered, the differences with respect to d-aug-cc-pV5Z are already below 10% when using the smallest basis set (aug-cc-pVDZ). Moreover, although the singly and doubly augmented cc-pVDZ basis sets present similar efficiency, d-aug-cc-pVTZ is clearly superior to aug-cc-pVTZ. DR_{SHS} is systematically underestimated no matter which basis set is used, which corresponds to an overestimation of the octupolar contribution (which was previously reported [37]). Its convergence with basis set size is consistent with that of β_{SHS}.

On the other hand, the basis set convergence of γ_{THS} is much slower than that of β_{SHS}. A clear difference between the singly and doubly augmented basis sets appears for the triple-ζ basis sets: γ_{THS} is underestimated by up to 25–30% with aug-cc-pVTZ, whereas the error is reduced to < 5% with d-aug-cc-pVTZ. A similar behavior with respect to adding diffuse functions has already been reported for the two-photon absorption cross section of water and has been explained by the contribution of very diffuse Rydberg excited states [58]. Moreover, differences with respect to d-aug-cc-pV5Z are still of the order of 10% when using aug-cc-pV5Z. A satisfactory (< 5% of difference) agreement requires d-aug-cc-pVTZ. When using singly-augmented basis sets, DR_{THS} is systematically overestimated (with relative errors of about 20% for the aug-cc-pV5Z basis set), whereas the opposite behavior is observed for the doubly augmented ones, but the amplitude of the underestimations is smaller. These basis set effects on both β_{SHS} and γ_{THS} are supported by an analysis

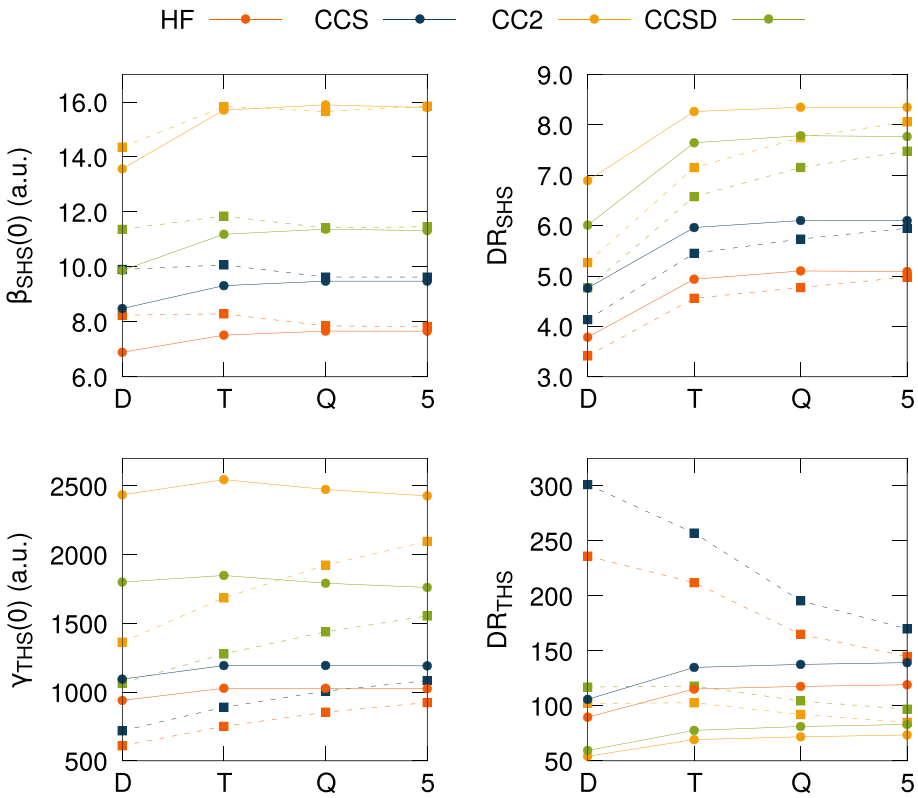

Fig. 3 Effect of the basis set (aug-cc-pVXZ, dashed lines and d-aug-cc-pVXZ, plain lines) and of the level of approximation on the first (above) and second (below) hyperpolarizabilities of water. Left panels report averaged quantities (β_{SHS}, γ_{THS}, a.u.), while right panels report the depolarization ratios

Table 1 Basis set and electron correlation effects on the static β_{SHS} (a.u.) and γ_{THS} (a.u.) of water (geometry from Ref. [40]) and on their depolarization ratios (DR)

	HF	CCS	CC2	CCSD
$\beta_{SHS}(0)$				
aug-cc-pVDZ	8.24 (7.6)	9.91 (4.5)	14.36 (− 9.1)	11.37 (0.4)
aug-cc-pVTZ	8.29 (8.2)	10.07 (6.2)	15.83 (0.2)	11.85 (4.7)
aug-cc-pVQZ	7.85 (2.5)	9.63 (1.5)	15.66 (− 0.9)	11.42 (0.9)
aug-cc-pV5Z	7.83 (2.3)	9.63 (1.6)	15.85 (0.3)	11.46 (1.3)
d-aug-cc-pVDZ	6.89 (− 10.1)	8.49 (− 10.5)	13.57 (− 14.1)	9.87 (− 12.7)
d-aug-cc-pVTZ	7.52 (− 1.9)	9.32 (− 1.7)	15.71 (− 0.6)	11.19 (− 1.1)
d-aug-cc-pVQZ	7.66 (0.0)	9.48 (0.0)	15.89 (0.6)	11.37 (0.5)
d-aug-cc-pV5Z	7.66	9.48	15.80	11.32
DR_{SHS}				
aug-cc-pVDZ	3.41 (− 33.0)	4.14 (− 32.1)	5.27 (− 36.9)	4.77 (− 38.7)
aug-cc-pVTZ	4.56 (− 10.5)	5.45 (− 10.6)	7.15 (− 14.3)	6.58 (− 15.4)
aug-cc-pVQZ	4.77 (− 6.3)	5.74 (− 5.9)	7.75 (− 7.2)	7.16 (− 7.9)
aug-cc-pV5Z	4.98 (− 2.3)	5.95 (− 2.4)	8.06 (− 3.4)	7.48 (− 3.7)
d-aug-cc-pVDZ	3.79 (− 25.7)	4.76 (− 21.9)	6.90 (− 17.4)	6.01 (− 22.6)
d-aug-cc-pVTZ	4.94 (− 3.1)	5.96 (− 2.2)	8.27 (− 1.0)	7.65 (− 1.6)
d-aug-cc-pVQZ	5.10 (0.2)	6.10 (0.1)	8.35 (0.1)	7.79 (0.2)
d-aug-cc-pV5Z	5.09	6.10	8.35	7.77
$\gamma_{THS}(0)$				
aug-cc-pVDZ	610 (− 40.5)	719 (− 39.6)	1363 (− 43.9)	1066 (− 39.5)
aug-cc-pVTZ	751 (− 26.7)	890 (− 25.3)	1686 (− 30.6)	1278 (− 27.4)
aug-cc-pVQZ	854 (− 16.7)	1008 (− 15.4)	1924 (− 20.7)	1439 (− 18.3)
aug-cc-pV5Z	924 (− 9.9)	1084 (− 9.0)	2097 (− 13.6)	1554 (− 11.8)
d-aug-cc-pVDZ	940 (− 8.3)	1095 (− 8.1)	2436 (0.4)	1801 (2.2)
d-aug-cc-pVTZ	1028 (0.3)	1193 (0.2)	2546 (4.9)	1849 (4.9)
d-aug-cc-pVQZ	1028 (0.3)	1194 (0.3)	2475 (1.9)	1792 (1.7)
d-aug-cc-pV5Z	1025	1191	2428	1762
DR_{THS}				
aug-cc-pVDZ	236 (98.0)	301 (116.2)	102 (38.9)	117 (40.9)
aug-cc-pVTZ	212 (77.9)	257 (84.6)	103 (39.7)	118 (42.1)
aug-cc-pVQZ	165 (38.5)	196 (40.4)	92 (25.4)	104 (25.7)
aug-cc-pV5Z	145 (21.8)	170 (22.3)	85 (16.1)	97 (16.2)
d-aug-cc-pVDZ	90 (− 24.8)	106 (− 24.0)	54 (− 26.3)	60 (− 28.4)
d-aug-cc-pVTZ	115 (− 3.3)	135 (− 3.1)	69 (− 5.7)	78 (− 6.5)
d-aug-cc-pVQZ	118 (− 1.2)	138 (− 1.2)	72 (− 2.3)	81 (− 2.3)
d-aug-cc-pV5Z	119	139	74	83

Relative differences (in %) with respect to d-aug-cc-pV5Z are given in parentheses

For aug-cc-pVXZ, the number of contracted GTOs (Gaussian Type Orbitals) is 41 ($X = D$), 92 ($X = T$), 172 ($X = Q$), and 287 ($X = 5$); for d-aug-cc-pVXZ, it is 58 ($X = D$), 126 ($X = T$), 229 ($X = Q$), 564 ($X = 5$)

of the different tensor components (Figs. S1 and S2), for which the convergence with respect to the basis set follows the same trend as for the average quantities.

The magnitude of both β_{SHS} and γ_{THS} responses as a function of electron correlation content follows a systematic trend: HF < CCS < CCSD < CC2. Employing the results obtained with the largest basis set, the HF and CCS levels underestimate the reference CCSD β_{SHS} (γ_{THS}) values by 32 and 16% (42 and 32%), respectively. On the other hand, CC2 overestimates both quantities, by 40% (38%) for the first (second) hyperpolarizability. These results are comparable to those reported for $\beta_{||}$ (although the error with respect to the largest basis set is larger for this EFISHG quantity) and $\gamma_{||}$ [40]. The dipolar contribution to DR_{SHS} increases from HF and CCS (34 and 16% of underestimation with respect to CCSD, for the largest basis set) to CC2 (7% of overestimation). The DR_{SHS} values satisfy the following ordering: HF < CCS < CCSD < CC2. The almost opposite order is

observed for DR_{THS}: CCS > HF > CCSD > CC2. Still, the differences with respect to CCSD are larger than in the case of DR_{SHS}: 68 and 48% of overestimation for CCS and HF, 11% of underestimation for CC2. Clearly, HF and CCS do not appear as reliable methods to predict DR_{THS} values.

The first and second hyperpolarizabilities of acetonitrile were computed at the HF, CCS, CC2, and CCSD levels with both the aug-cc-pVTZ and d-aug-cc-pVTZ basis sets (Tables 2 and S1 and Fig. 4). For β_{SHS}, the differences between these two basis sets are similar to those observed for the water case discussed above. For γ_{SHS}, the basis set effects are smaller (smaller than 4%), underlying the cooperation effects between basis functions on different atomic centers. The effects of adding a second set of diffuse functions on the depolarization ratio are larger for the second than for the first hyperpolarizability responses. With respect to the reference CCSD/d-aug-cc-pVTZ values, frequency dispersion effects on β_{SHS} are generally slightly overestimated when using the aug-cc-pVTZ basis set as well as when adopting the CCS and CC2 levels of approximation. These effects get smaller when going from SHS to THS quantities. Electron correlation effects are substantial on β_{SHS} of acetonitrile, with an increase by a factor of 3 between CCS (and HF) and CCSD (and CC2) (together with an increase in the depolarization ratio from octupolar at the HF and CCS level to dipolar at the CC2 and CCSD level). On the other hand, the differences between the CC2 and CCSD β_{SHS} and γ_{SHS} values are much smaller than for water. Moreover, the CCS method strongly underestimates (overestimates) the CCSD DR_{SHS} (DR_{THS}) values.

4.2 SHS and THS of 6 reference molecules

Based on the results of the previous section, the CCSD/d-aug-cc-pVDZ level of approximation has been used to calculate the static and dynamic first and second hyperpolarizabilities of the whole set of 6 reference molecules (Tables 3, 4). As previously reported [37], this set of molecules spreads over a broad range of dipolar/octupolar character, as evidenced by DR_{SHS} values ranging from 1.5 (octupolar CCl_4 molecule) to *circa* six (dipolar, H_2O and CH_3CN molecules). The octupolar contribution dominates the β_{SHS} value of chlorinated methanes (since $\rho_{3/1} > 1$), especially in the case of chloroform and dichloromethane. In the CH_xCl_y series, $CHCl_3$ presents the largest β_{SHS} value, followed by CCl_4, which has no dipolar contribution, and then the CH_2Cl_2 and CH_3Cl molecules. The acetonitrile displays a large β response, due its dipolar contribution (originating from the cyano group).

Table 2 Basis set and electron correlation effects on the static and dynamic (1500, 1300 and 1064 nm) β_{SHS} (a.u.) and γ_{THS} (a.u.) of acetonitrile, with their corresponding depolarization ratios (DR)

	d-aug-cc-pVDZ[a]				d-aug-cc-pVTZ			
	HF	CCS	CC2	CCSD	HF	CCS	CC2	CCSD
$\beta_{SHS}(-2\omega;\omega,\omega)$								
Static	6.42 (− 2.7)	4.42 (− 9.3)	17.26 (2.4)	16.74 (6.8)	6.59	4.83	16.84	15.61
1500 nm	6.65 (− 2.4)	4.52 (− 8.8)	17.91 (2.6)	17.41 (6.9)	6.81	4.92	17.45	16.21
1300 nm	6.73 (− 2.3)	4.56 (− 8.7)	18.14 (2.6)	17.64 (6.9)	6.88	4.96	17.66	16.42
1064 nm	6.89 (− 2.1)	4.64 (− 8.3)	18.59 (2.7)	18.11 (7.0)	7.03	5.02	18.09	16.84
DR_{SHS}								
Static	2.53 (10.1)	1.52 (1.4)	5.96 (9.8)	5.87 (11.7)	2.27	1.50	5.38	5.18
1500 nm	2.58 (10.3)	1.54 (2.2)	5.92 (9.7)	5.84 (11.6)	2.31	1.50	5.35	5.16
1300 nm	2.60 (10.4)	1.54 (2.5)	5.90 (9.6)	5.82 (11.5)	2.33	1.50	5.33	5.15
1064 nm	2.64 (10.5)	1.55 (3.1)	5.87 (9.5)	5.80 (11.4)	2.36	1.51	5.31	5.14
$\gamma_{THS}(-3\omega;\omega,\omega,\omega)$								
Static	2986 (− 2.6)	3559 (− 3.0)	4577 (3.1)	4037 (3.2)	3064	3664	4435	3907
1500 nm	3256 (− 2.5)	3862 (− 2.9)	5030 (3.4)	4420 (3.5)	3339	3973	4860	4263
1300 nm	3355 (− 2.5)	3972 (− 2.8)	5196 (3.5)	4558 (3.6)	3439	4084	5014	4392
1064 nm	3562 (− 2.5)	4203 (− 2.8)	5548 (3.7)	4853 (3.9)	3650	4319	5342	4666
DR_{THS}								
Static	156 (− 42.9)	175 (− 45.1)	56 (− 15.9)	70 (− 22.1)	223	253	65	85
1500 nm	153 (− 40.1)	170 (− 42.4)	54 (− 14.8)	67 (− 20.7)	214	243	62	81
1300 nm	152 (− 39.2)	169 (− 41.6)	53 (− 14.4)	66 (− 20.3)	211	239	61	80
1064 nm	149 (− 37.4)	167 (− 39.9)	51 (− 13.8)	64 (− 19.4)	205	233	58	77

Relative errors with respect to d-aug-cc-pVTZ (right) are given in parentheses for the d-aug-cc-pVDZ (left) values

[a]For d-aug-cc-pVXZ: 135 ($X = D$) and 282 ($X = T$) contracted GTOs are used

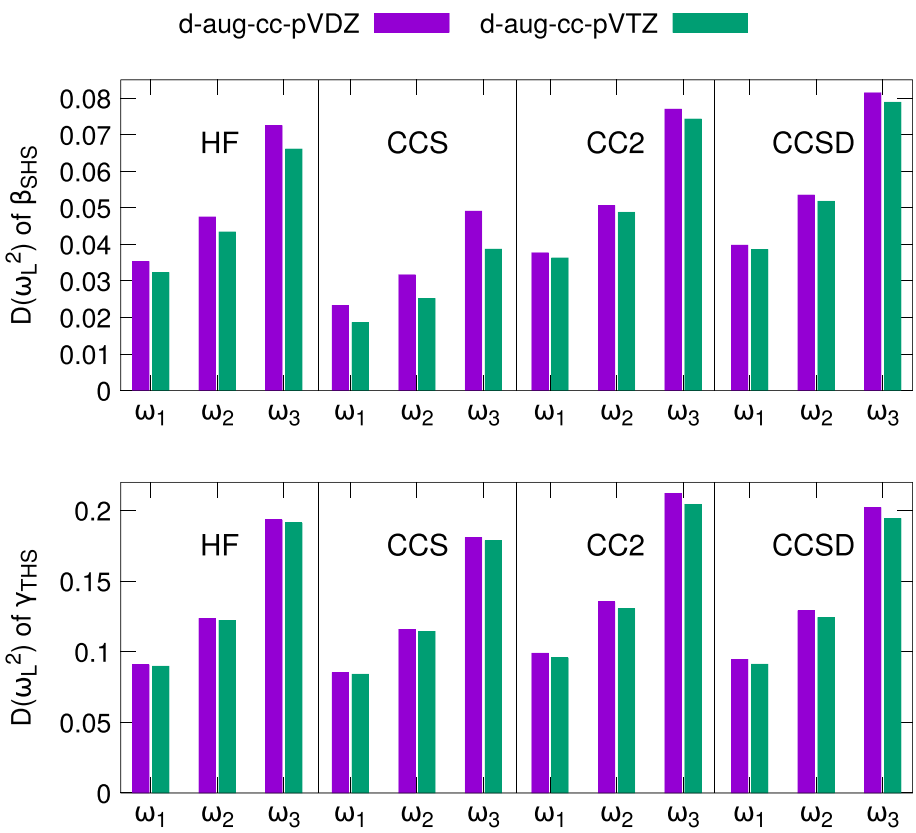

Fig. 4 Effect of the electron correlation and basis set on the frequency dispersion $\left[D\left(\omega_L^2\right)\right]$ of the first (β_{SHS}) and second (γ_{THS}) hyperpolarizabilities of acetonitrile ($\omega_1 = 1500$ nm, $\omega_2 = 1300$ nm, and $\omega_3 = 1064$ nm)

Table 3 CCSD/d-aug-cc-pVDZ static SHS and THS responses for the six reference molecules: β_{SHS} (a.u.) and γ_{THS} (a.u.), their depolarization ratios (DR), their spherical tensor decompositions, and the corresponding nonlinear anisotropy parameters

	CCl_4	CH_2Cl_2	$CHCl_3$	CH_3Cl	CH_3CN	H_2O
β_{SHS}	15.63	13.41	16.32	12.32	16.74	9.87
$\mathrm{DR}_{\mathrm{SHS}}$	1.50	1.53	1.57	2.94	5.87	6.01
$\lvert\beta_{J=1}\rvert$	~ 0	3.67	6.59	18.22	32.71	19.40
$\lvert\beta_{J=3}\rvert$	50.65	43.09	51.91	28.61	21.14	12.06
$\rho_{3/1}$	$\sim \infty$	11.75	7.88	1.57	0.65	0.62
γ_{THS}	12,719	8474	10,993	5065	4037	1801
$\mathrm{DR}_{\mathrm{THS}}$	5744	90	169	414	70	60
$\mathrm{DR}'_{\mathrm{THS}}$	$\sim \infty$	94	176	440	72	61
$\lvert\gamma_{J=0}\rvert$	28,434	18,296	24,130	11,241	8623	3813
$\lvert\gamma_{J=2}\rvert$	~ 0	5923	5638	1647	3221	1565
$\lvert\gamma_{J=4}\rvert$	1332	1522	1412	475	680	263
$\rho_{0/2}$	$\sim \infty$	3.089	4.280	6.823	2.677	2.437
$\rho_{4/2}$	$\sim \infty$	0.257	0.250	0.288	0.211	0.168

The γ responses vary over a broader range of amplitudes, with γ_{THS} of CCl_4 150% larger than in CH_3Cl. With its four polarizable chlorine atoms, CCl_4 possesses the largest γ_{THS} response and each time a chlorine atom is replaced by an hydrogen atom, γ_{THS} decreases by about 20%. The smaller γ_{THS} values of acetonitrile and water are explained by their correspondingly lower $J = 0$ contribution. For all compounds, the isotropic component is in fact dominant, followed by the quadrupolar contribution (except for CCl_4, where it is zero by symmetry). Therefore, γ_{THS} is governed by the $\langle\gamma^2_{ZZZZ}\rangle$ term (Eq. 19), all $\rho_{0/2}$ values are larger than 1, and all $\rho_{4/2}$ values are smaller than 1 (the $\rho_{4/2}$ values are far from the hexadecapolar limit).

These analyses are confirmed for the dynamic quantities (Table 4) because the photon energies of the second and third harmonics are still far from the electronic resonances of the molecules. Indeed, for a wavelength of 1064 nm, the third harmonics photons have an energy close to 3.5 eV, while the

Table 4 Static and dynamic (1500, 1300 and 1064 nm) β_{SHS} (a.u.) and γ_{THS} (a.u.) of the six reference compounds, together with their depolarization ratios (DR) in parentheses, as obtained at the CCSD/d-aug-cc-pVDZ level

	CCl_4	CH_2Cl_2	$CHCl_3$	CH_3Cl	CH_3CN	H_2O
$\beta_{SHS}(-2\omega;\omega,\omega)$ (DR_{SHS})						
Static	15.63 (1.50)	13.41 (1.53)	16.32 (1.57)	12.32 (2.94)	16.74 (5.87)	9.87 (6.01)
1500 nm	16.28 (1.50)	14.22 (1.54)	17.12 (1.57)	13.25 (2.96)	17.41 (5.84)	10.29 (6.22)
1300 nm	16.50 (1.50)	14.51 (1.54)	17.40 (1.57)	13.59 (2.97)	17.64 (5.82)	10.43 (6.30)
1064 nm	16.97 (1.50)	15.11 (1.54)	17.99 (1.57)	14.27 (2.98)	18.11 (5.80)	10.73 (6.46)
$\gamma_{THS}(-3\omega;\omega,\omega,\omega)$ (DR_{THS})						
Static	12,719 (5744)	8474 (90)	10,993 (169)	5065 (414)	4037 (70)	1801 (60)
1500 nm	14,279 (5451)	9575 (85)	12,389 (161)	5672 (454)	4420 (67)	2027 (48)
1300 nm	14,859 (5358)	9989 (84)	12,910 (158)	5899 (471)	4558 (66)	2113 (44)
1064 nm	16,118 (5182)	10,892 (80)	14,044 (152)	6394 (512)	4853 (64)	2304 (38)

first excitation energy is, at least, twice larger (for example, it amounts to 7.4 eV in the case of water [59]).

For the three wavelengths considered, frequency dispersion (Table S2) remains (i) between 8 and 16% for β_{SHS} (at 1064 nm the ordering of the $D(\omega_L^2)$ values satisfies $CH_3CN \approx CCl_4 \approx H_2O < CHCl_3 < CH_2Cl_2 < CH_3Cl$) and (ii) between 20 and 30% for γ_{THS} ($CH_3CN < CCl_4 \approx CH_3Cl < CHCl_3 \approx H_2O < CH_2Cl_2$). The frequency dispersion has a negligible effect on DR_{SHS}, with the exception of water where the increase attains 7% for 1064 nm. The variations are larger for DR_{THS}, of about 10% at 1064 nm, except for chloromethane and water (24 and 36%, respectively). These DR_{THS} variations are associated with an increase of the quadrupolar (hexacapolar) contribution for water (chloromethane).

Though experiments have been carried out in solutions, it is interesting to see how good is the agreement with the CCSD γ_{THS} values obtained for the isolated molecule. This comparison is achieved for a wavelength of 1300 nm, employed in Ref. [11]. Note that in the latter reference, the B-convention was adopted so that their γ_{THS} values have been multiplied by a factor of 6 to match with the T-convention. For acetonitrile, the experimental value (68×10^2 a.u.) is about 30% larger than our CCSD prediction (46×10^2 a.u., Table 4). The agreement is however much better for dichloromethane (exp. value of 111×10^2a.u. vs 100×10^2a.u. at the CCSD level), chloroform (126×10^2 a.u. vs 129×10^2a.u. at the CCSD level), and carbon tetrachloride (152×10^2 a.u. vs 149×10^2 a.u. at the CCSD level), with differences with respect to the CCSD values of 10% or less. These good agreements suggest that the Liq/Gas ratios are close to one, at least for the chlorinated species. This contrasts with what has been observed for the β_{SHS} response [37].

5 Conclusions

The static and dynamic second harmonic (β_{SHS}) and third harmonic (γ_{THS}) scattering hyperpolarizabilities of water, carbon tetrachloride, chloroform, dichloromethane, chloromethane, and acetonitrile have been evaluated by using a hierarchy of coupled cluster response methods in combination with atomic basis sets of increasing size. The focus of this paper goes beyond the prediction of benchmark β_{SHS} and γ_{THS} quantities and deals with the depolarization ratios as well as with the decomposition of the rank-3 and rank-4 tensors into their spherical invariants (dipolar and octupolar for β_{SHS}, isotropic, quadrupolar, and hexadecapolar for γ_{THS}). To our knowledge, this is the first quantum chemical investigation of γ_{THS}, following two recent papers on their measurements [11, 12]. Substantial electron correlation and basis set effects are evidenced and depend on the nature of the molecule. On the basis of a detailed investigation of the second- and third-order responses of water and acetonitrile, the CCSD/d-aug-cc-pVDZ level has been selected to study the chlorinated methane derivatives. CCSD results demonstrate that γ_{THS} of these compounds is dominated by its isotropic component, while the second largest contribution is the quadrupolar one (with the exception of carbon tetrachloride, where it is zero). In the case of β_{SHS}, its dipolar character increases from carbon tetrachloride to chloromethane. Comparisons with experimental data obtained from measurements in liquid phase show that the increase of γ_{THS} with the number for chlorine atoms is well reproduced by the calculations. These comparisons also suggest that the solvation effects are smaller for γ_{THS} than for β_{SHS}.

Acknowledgements At the occasion of his 60th birthday, it is a pleasure to dedicate this paper to Prof. Antonio RIZZO, who is pioneering since several decades the evaluation of high-order optical effects and

their confrontation with experiment, leading to an improved understanding of the interactions between light and matter. This work was supported by funds from the Francqui Foundation. The calculations were performed on the computers of the Consortium des Équipements de Calcul Intensif, including those of the Technological Platform of High-Performance Computing, for which we gratefully acknowledge the financial support of the FNRS-FRFC (Convention Nos. 2.4.617.07.F and 2.5020.11) and of the University of Namur.

References

1. Franken PA, Hill AE, Peters CW, Weinreich G (1961) Phys Rev Lett 7:118–119. https://doi.org/10.1103/PhysRevLett.7.118
2. Terhune RW, Maker PD, Savage CM (1962) Phys Rev Lett 8:404–406. https://doi.org/10.1103/PhysRevLett.8.404
3. Verbiest T, Clays K, Rodriguez V (2009) Second-order nonlinear optical characterization techniques: an introduction. Taylor & Francis, Abington-on-Thames
4. Kanis DR, Ratner MA, Marks TJ (1994) Chem Rev 94:195–242. https://doi.org/10.1021/cr00025a007
5. Bredas JL, Adant C, Tackx P, Persoons A, Pierce BM (1994) Chem Rev 94:243–278. https://doi.org/10.1021/cr00025a008
6. Shelton DP, Rice JE (1994) Chem Rev 94:3–29. https://doi.org/10.1021/cr00025a001
7. Bishop DM, Norman P (2001) In: Nalwa HS (ed) Handbook of advanced electronic and photonic materials and devices. Academic Press, San Diego, pp 1–62
8. Champagne B, Kirtman P (2001) In: Nalwa HS (ed) Handbook of advanced electronic and photonic materials and devices. Academic Press, San Diego, pp 63–127
9. Papadopoulos MG, Sadlej AJ, Leszczynski J (2006) Non-linear optical properties of matter: from molecules to condensed phases. Springer, Dordrecht OCLC: 72145327
10. Castet F, Rodriguez V, Pozzo JL, Ducasse L, Plaquet A, Champagne B (2013) Acc Chem Res 46:2656–2665. https://doi.org/10.1021/ar4000955
11. Van Steerteghem N, Clays K, Verbiest T, Van Cleuvenbergen S (2017) Anal Chem 89:2964–2971. https://doi.org/10.1021/acs.analchem.6b04429
12. Rodriguez V (2017) J Phys Chem C 121:8510–8514. https://doi.org/10.1021/acs.jpcc.7b00983
13. Clays K, Persoons A (1991) Phys Rev Lett 66:2980–2983. https://doi.org/10.1103/PhysRevLett.66.2980
14. Heesink GJT, Ruiter AGT, van Hulst NF, Bölger B (1993) Phys Rev Lett 71:999–1002. https://doi.org/10.1103/PhysRevLett.71.999
15. Hendrickx E, Clays K, Persoons A (1998) Acc Chem Res 31:675–683. https://doi.org/10.1021/ar960233o
16. Shelton DP (2012) J Chem Phys 137:044312. https://doi.org/10.1063/1.4738897
17. Ostroverkhov V, Petschek RG, Singer KD, Sukhomlinova L, Twieg RJ, Wang SX, Chien LC (2000) J Opt Soc Am B 17:1531–1542. https://doi.org/10.1364/JOSAB.17.001531
18. Mançois F, Sanguinet L, Pozzo JL, Guillaume M, Champagne B, Rodriguez V, Adamietz F, Ducasse L, Castet F (2007) J Phys Chem B 111:9795–9802. https://doi.org/10.1021/jp073386+
19. Duncan T, Song K, Hung ST, Miloradovic I, Nayak A, Persoons A, Verbiest T, Therien M, Clays K (2008) Angew Chem Int Ed 120:3020–3023. https://doi.org/10.1002/ange.200703187
20. Asselberghs I, Flors C, Ferrighi L, Botek E, Champagne B, Mizuno H, Ando R, Miyawaki A, Hofkens J, Auweraer MVd, Clays K (2008) J Am Chem Soc 130:15713–15719. https://doi.org/10.1021/ja805171q
21. Garrett K, Sosa Vazquez X, Egri SB, Wilmer J, Johnson LE, Robinson BH, Isborn CM (2014) J Chem Theor Comput 10:3821–3831. https://doi.org/10.1021/ct500528z
22. Quertinmont J, Champagne B, Castet F, Hidalgo Cardenuto M (2015) J Phys Chem A 119:5496–5503. https://doi.org/10.1021/acs.jpca.5b00631
23. Beaujean P, Bondu F, Plaquet A, Garcia-Amors J, Cusido J, Raymo FM, Castet F, Rodriguez V, Champagne B (2016) J Am Chem Soc 138:5052–5062. https://doi.org/10.1021/jacs.5b13243
24. Coe BJ, Foxon SP, Pilkington RA, Sánchez S, Whittaker D, Clays K, Van Steerteghem N, Brunschwig BS (2016) Organometallics 35:3014–3024. https://doi.org/10.1021/acs.organomet.6b00536
25. Bishop DM (1994) In: Sabin JR, Zerner MC (eds) Advances in quantum chemistry, vol 25. Academic Press, San Diego, pp 1–45. https://doi.org/10.1016/S0065-3276(08)60017-9
26. Maroulis G (1991) J Chem Phys 94:1182–1190. https://doi.org/10.1063/1.460025
27. Sekino H, Bartlett RJ (1993) J Chem Phys 98:3022–3037. https://doi.org/10.1063/1.464129
28. Bishop DM, Norman P (1999) J Chem Phys 111:3042–3050. https://doi.org/10.1063/1.479661
29. Rizzo A, Coriani S, Fernàndez B, Christiansen O (2002) Phys Chem Chem Phys 4:2884–2890. https://doi.org/10.1039/b109689c
30. Luis JM, Reis H, Papadopoulos M, Kirtman B (2009) J Chem Phys 131:034116. https://doi.org/10.1063/1.3171615
31. Maroulis G, Menadakis M (2010) Chem Phys Lett 494:144–149. https://doi.org/10.1016/j.cplett.2010.06.006
32. Dutra AS, Castro MA, Fonseca TL, Fileti EE, Canuto S (2010) J Chem Phys 132:034307. https://doi.org/10.1063/1.3298914
33. Bast R, Ekström U, Gao B, Helgaker T, Ruud K, Thorvaldsen AJ (2011) Phys Chem Chem Phys 13:2627–2651. https://doi.org/10.1039/C0CP01647K
34. Bulik IW, Zaleśny R, Bartkowiak W, Luis JM, Kirtman B, Scuseria GE, Avramopoulos A, Reis H, Papadopoulos MG (2013) J Comput Chem 34:1775–1784. https://doi.org/10.1002/jcc.23316
35. Coe JP, Paterson MJ (2014) J Chem Phys 141:124118. https://doi.org/10.1063/1.4896229
36. Zaleśny R, Baranowska-Łaczkowska A, Medved' M, Luis JM (2015) J Chem Theor Comput 11:4119–4128. https://doi.org/10.1021/acs.jctc.5b00434
37. Castet F, Bogdan E, Plaquet A, Ducasse L, Champagne B, Rodriguez V (2012) J Chem Phys 136:024506. https://doi.org/10.1063/1.3675848
38. Castet F, Champagne B (2012) J Chem Theor Comput 8:2044–2052. https://doi.org/10.1021/ct300174z
39. de Wergifosse M, Castet F, Champagne B (2015) J Chem Phys 142:194102. https://doi.org/10.1063/1.4920977
40. Beaujean P, Champagne B (2016) J Chem Phys 145:044311. https://doi.org/10.1063/1.4958736
41. Bishop DM, Kirtman B, Kurtz HA, Rice JE (1993) J Chem Phys 98:8024–8030. https://doi.org/10.1063/1.464556
42. Bishop DM, Gu FL, Cybulski SM (1998) J Chem Phys 109:8407–8415. https://doi.org/10.1063/1.477503
43. Andrews D (1980) J Phys B 13:4091–4099. https://doi.org/10.1088/0022-3700/13/20/021
44. Andrews DL, Thirunamachandran T (1977) J Chem Phys 67:5026. https://doi.org/10.1063/1.434725
45. Terhune RW, Maker PD, Savage CM (1965) Phys Rev Lett 14:681–684. https://doi.org/10.1103/PhysRevLett.14.681
46. Cyvin SJ, Rauch JE, Decius JC (1965) J Chem Phys 43:4083. https://doi.org/10.1063/1.1696646
47. Bersohn R, Pao Y, Frisch HL (1966) J Chem Phys 45:3184–3198. https://doi.org/10.1063/1.1728092
48. Jerphagnon J, Chemla D, Bonneville R (1978) Adv Phys 27:609–650. https://doi.org/10.1080/00018737800101454

49. Alexiewicz W, Ożgo Z, Kielich S (1975) Acta Phys Pol A 48:243
50. Tadeusz B, Zdzislaw O (2010) J Comput Methods Sci Eng https://doi.org/10.3233/JCM-2010-0314
51. Brasselet S, Zyss J (1998) J Opt Soc Am B 15:257. https://doi.org/10.1364/JOSAB.15.000257
52. Aidas K, Angeli C, Bak KL, Bakken V, Bast R, Boman L, Christiansen O, Cimiraglia R, Coriani S, Dahle P, Dalskov EK, Ekström U, Enevoldsen T, Eriksen JJ, Ettenhuber P, Fernández B, Ferrighi L, Fliegl H, Frediani L, Hald K, Halkier A, Hättig C, Heiberg H, Helgaker T, Hennum AC, Hettema H, Hjertenæs E, Høst S, Høyvik IM, Iozzi MF, Jansík B, Jensen HJAa, Jonsson D, Jørgensen P, Kauczor J, Kirpekar S, Kjærgaard T, Klopper W, Knecht S, Kobayashi R, Koch H, Kongsted J, Krapp A, Kristensen K, Ligabue A, Lutnæs OB, Melo JI, Mikkelsen KV, Myhre RH, Neiss C, Nielsen CB, Norman P, Olsen J, Olsen JMH, Osted A, Packer MJ, Pawlowski F, Pedersen TB, Provasi PF, Reine S, Rinkevicius Z, Ruden TA, Ruud K, Rybkin VV, Sałek P, Samson CCM, Merás ASde, Saue T, Sauer SPA, Schimmelpfennig B, Sneskov K, Steindal AH, Sylvester-Hvid KO, Taylor PR, Teale AM, Tellgren EI, Tew DP, Thorvaldsen AJ, Thøgersen L, Vahtras O, Watson MA, Wilson DJD, Ziolkowski M, Ågren H, (2014) WIREs Comput Mol Sci 4:269–284. https://doi.org/10.1002/wcms.1172
53. Hättig C (1998) Chem Phys Lett 296:245–252. https://doi.org/10.1016/S0009-2614(98)01004-5
54. Hättig C, Jørgensen P (1999) Adv Quantum Chem 35:111–148. https://doi.org/10.1016/S0065-3276(08)60458-X
55. Christiansen O, Gauss J, Stanton JF (1999) Chem Phys Lett 305:147–155. https://doi.org/10.1016/S0009-2614(99)00358-9
56. Helgaker T, Coriani S, Jørgensen P, Kristensen K, Olsen J, Ruud K (2012) Chem Rev 112:543
57. Dunning TH (1989) J Chem Phys 90:1007. https://doi.org/10.1063/1.456153
58. Paterson MJ, Christiansen O, Pawłowski F, Jørgensen P, Hättig C, Helgaker T, Sałek P (2006) J Chem Phys 124:054322. https://doi.org/10.1063/1.2163874
59. Chutjian A, Hall RI, Trajmar S (1975) J Chem Phys 63:892–898. https://doi.org/10.1063/1.431370